REPORT DOCUMENTATION PAGE

Form Approved OMB No. 074-0188

1. AGENCY USE ONLY (Leave blank)	2. REPORT DATE Feb.1996	3. REPORT TYPE AND DATES COVERED Technical Report

4. TITLE AND SUBTITLE

Analysis of the Results of the Trans-Arctic Propagation Experiment

5. FUNDING NUMBERS

N/A

6. AUTHOR(S)

A.N. Gavrilov, & M. Yu. Andreyev

7. PERFORMING ORGANIZATION NAME(S) AND ADDRESS(ES)

Marine Science International Corporation

8. PERFORMING ORGANIZATION REPORT NUMBER

MSIC Report No.2/96

9. SPONSORING / MONITORING AGENCY NAME(S) AND ADDRESS(ES)

SERDP
901 North Stuart St. Suite 303
Arlington, VA 22203

10. SPONSORING / MONITORING AGENCY REPORT NUMBER

N/A

11. SUPPLEMENTARY NOTES

Information available from Marine Science International Corporation, MSIC Report No.2/96, February 1996.

12a. DISTRIBUTION / AVAILABILITY STATEMENT

Approved for public release: distribution is unlimited

12b. DISTRIBUTION CODE

A

13. ABSTRACT ***(Maximum 200 Words)***

The Transarctic Acoustic Propagation (TAP) experiment has been carried out in April 1994. During the 5 days of the experiment, thirty-one CW and twelve broadband acoustic signals lasting 1 hour were transmitted at 19.6 Hz from ice camp TURPAN as it drifted 300 km north of Spitsbergen, over 2600 km to the ice camp SIMI in the Beaufort Sea, and 900 km to the ice camp NARWHAL in the Lincoln Sea. The main goal of the experiment was to explore the feasibility of long-range long-term acoustic transmissions in the Arctic Ocean for monitoring climatic changes in the ocean temperature and the ice cover.

14. SUBJECT TERMS

Acoustic propagation, Climatic change, Ocean temperature, SERDP

15. NUMBER OF PAGES 61

16. PRICE CODE N/A

17. SECURITY CLASSIFICATION OF REPORT	18. SECURITY CLASSIFICATION OF THIS PAGE	19. SECURITY CLASSIFICATION OF ABSTRACT	20. LIMITATION OF ABSTRACT
unclass.	unclass.	unclass.	UL

MARINE SCIENCE INTERNATIONAL CORPORATION

INTERANNUAL VARIABILITY OF THE ATLANTIC WATER IN THE ARCTIC BASIN

S.V. Pisarev

ANALYSIS OF THE RESULTS OF THE TRANS-ARCTIC PROPAGATION EXPERIMENT (Transmissions from i/c TURPAN to i/c NARWHAL)

A. N. Gavrilov
M. Yu. Andreyev

MSIC Report No. 2/96

1996

ANALYSIS OF THE RESULTS OF THE TRANS-ARCTIC PROPAGATION EXPERIMENT (Transmissions from i/c TURPAN to i/c NARWHAL) .

A. N. Gavrilov
M. Yu. Andreyev

TABLE OF CONTENTS

LIST OF FIGURES

LIST OF TABLES

I. INTRODUCTION

The Transarctic Acoustic Propagation (TAP) experiment has been carried out in April 1994. During the 5 days of the experiment, thirty-one CW and twelve broadband acoustic signals lasting 1 hour were transmitted at 19.6 Hz from ice camp TURPAN as it drifted 300 km north of Spitsbergen, over 2600 km to the ice camp SIMI in the Beaufort Sea, and 900 km to the ice camp NARWHAL in the Lincoln Sea. The main goal of the experiment was to explore the feasibility of long-range long-term acoustic transmissions in the Arctic Ocean for monitoring climatic changes in the ocean temperature and the ice cover.

The results of the processing and analysis of the TAP signals received at SIMI have been published in several papers [1-3], while the signals received at NARWHAL, have not been analyzed in all details so far. The characteristics of the acoustic propagation from TURPAN to NARWHAL should be of particular interest for the ACOUS program [1], because the first receiving array planned for year-round acoustic transmissions in the framework of this program, is expected to be deployed in the Lincoln Sea, not far from the NARWHAL location.

In the first part of the report we discuss the environmental conditions, the results of primary processing of the signals, and some issues concerning the array calibration and array echo-locating system.

Final processing of the TAP signals received at NARWHAL was aimed, first of all, at mode filtering on a vertical array, and determination of the modal transmission loss, because those data are necessary for planning the acoustic power capacity of the source required for year-round transmissions across the Arctic Ocean to the Lincoln Sea. In this report we consider, mainly, the results of processing of the broadband signals. The experimental results on both the modal propagation loss and travel times are compared with the results of theoretical modeling.

II. EXPERIMENTAL CONDITIONS

Location of the Transmitting and Receiving Sites

Figure 1 illustrates the relative location of the transmitter and receiver sites in the TAP experiment. In this plane chart the great blank rectangles show the relative bearings of the particular maps in Figures 2-4 (northward oriented in an upward direction) which demonstrate the drift charts of the ice camps TURPAN, SIMI and NARWHAL.

The drift chart of the transmitting camp, TURPAN, in Figure 2 has been created using 2600 GPS readings taken with a 1 minute step. Note the break in the GPS measurements on the 19th of April (digit marks in the maps indicate the day of April, 1994.). The map scale in Figure 2 is the largest, because TURPAN drifted much faster than the receiving ice camps.

The drift of SIMI sketched out by 12000 GPS readings with a 1 second step, is shown in Figure 3. Note an abrupt change in the drift on April 1st – after a stop the ice camp started drifting more quickly to the East.

At NARWHAL, the GPS data were recorded with a 1 hour sampling period. Therefore, the NARWHAL's drift (Figure 4) has been drafted using only 140 GPS readings. Note that there was no noticeable movement of the ice camp until 6 p.m. April, 19th.

The distances between TURPAN and the receiving camps, SIMI and NARWHAL, were calculated from the system of differential equations for the geodesics on the Earth surface [1]:

$$\theta' = \frac{\cos(\alpha)}{\mu(\theta)},$$

$$\varphi' = \frac{\sin(\alpha)}{\nu(\theta)\cos(\theta)},$$

$$\alpha' = \frac{\sin(\alpha)}{\nu(\theta)}\tan(\theta),$$

where

$$\mu(\theta) = \frac{r_{eq}\left(1-\varepsilon^2\right)}{\left(1-\varepsilon^2\sin^2\theta\right)^{3/2}},$$

$$\nu(\theta) = \frac{r_{eq}}{\left(1-\varepsilon^2\sin^2\theta\right)^{1/2}}$$

Here is given mean differentiation with respect to the arc length along the geodesic; r_{eq} and r_p are the equatorial and polar Earth radii, and $\varepsilon^2 = 1 - r_p^2/r_{eq}^2$. We used the 84 WKS model of the geoid with r_{eq} = 6378137 m and r_p = 6356752 m. Numerical integration of this system of ordinary differential equations was performed with the use of the 4th order Runge-Kutta formulas.

Figure 5 displays the time dependence (the hours counted from midnight, April, 17th) of the distance from TURPAN to both of the receiving camps. The range to NARWHAL was less changeable than that to SIMI. The maximal velocity of TURPAN relative to NARWHAL was less then 300 m/h, whereas that to SIMI exceeded 500 m/h.

Environment

The bottom profile from TURPAN to NARWHAL at the beginning and the end of the TAP transmissions is shown in Figure 6. This bathymetry chart was drawn from the 5-minute topographic grid of the Earth's surface. It is necessary to note that the bathymetric map of the Lincoln Sea presented in [2], and the bottom profile along the TURPAN-NARWHAL path given in [3] (dotted line in Figure 6), demonstrate the continental slope at the northern edge of the Lincoln Sea to be much steeper than that followed from the 5-minute bathymetry data.

The sound speed profiles measured at TURPAN and ~~SIMI~~ NARWHAL are given in Figures 7 and 8.

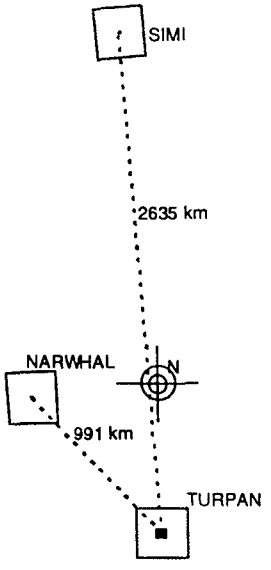

Fig.1. Relative positions of the transmitting and receiving sites in the TAP experiment

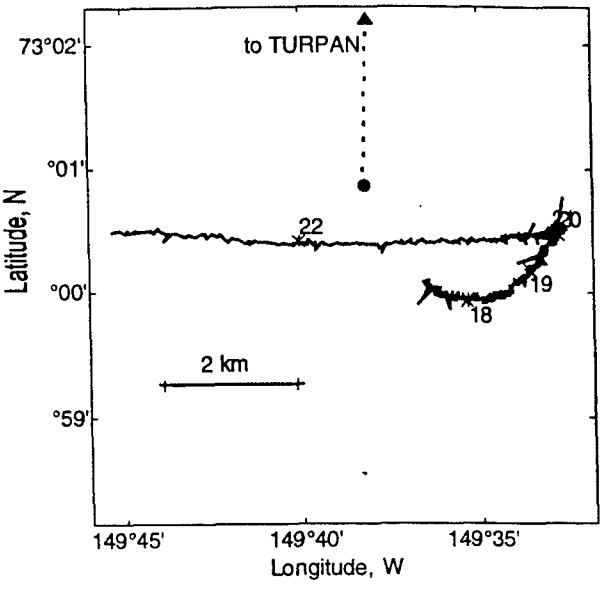

Fig.2. Chart of the SIMI drift

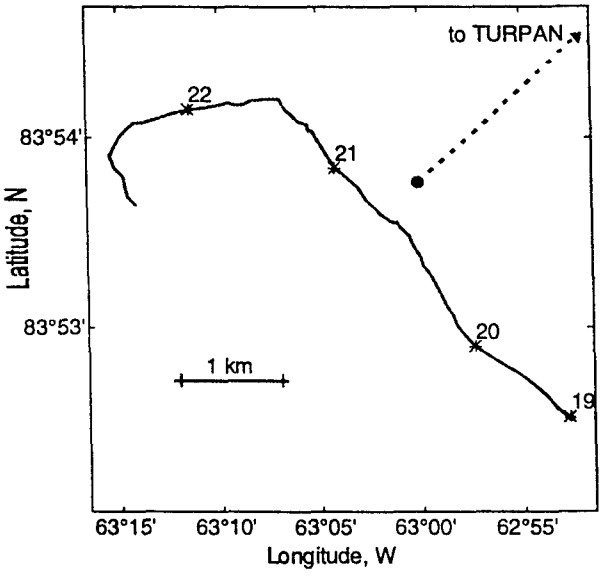

Fig.3. Chart of the NARWHAL drift

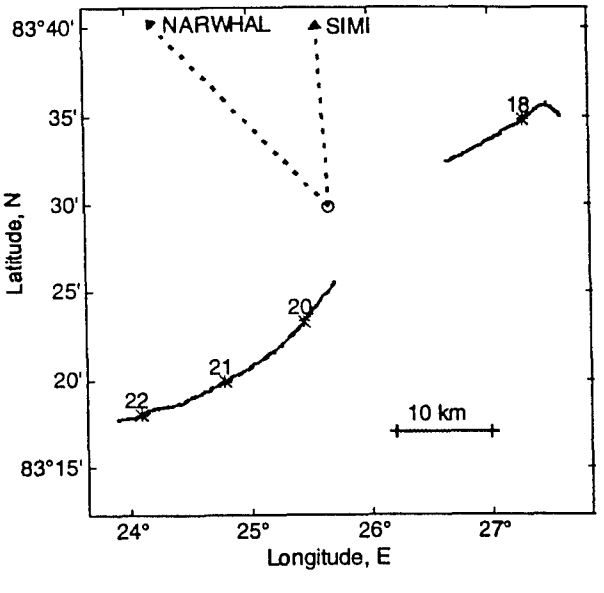

Fig.4. Chart of the TURPAN drift

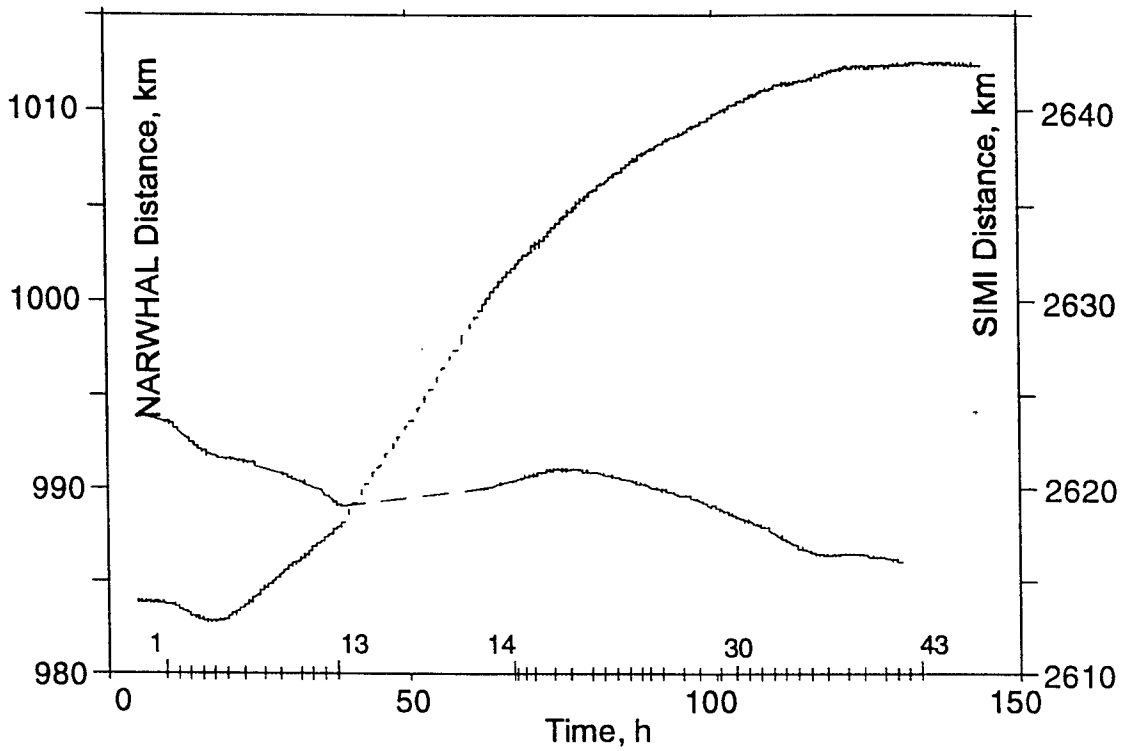

Fig.5. TURPAN-NARWHAL and TURPAN-SIMI distances (1-43 - transmission numbers)

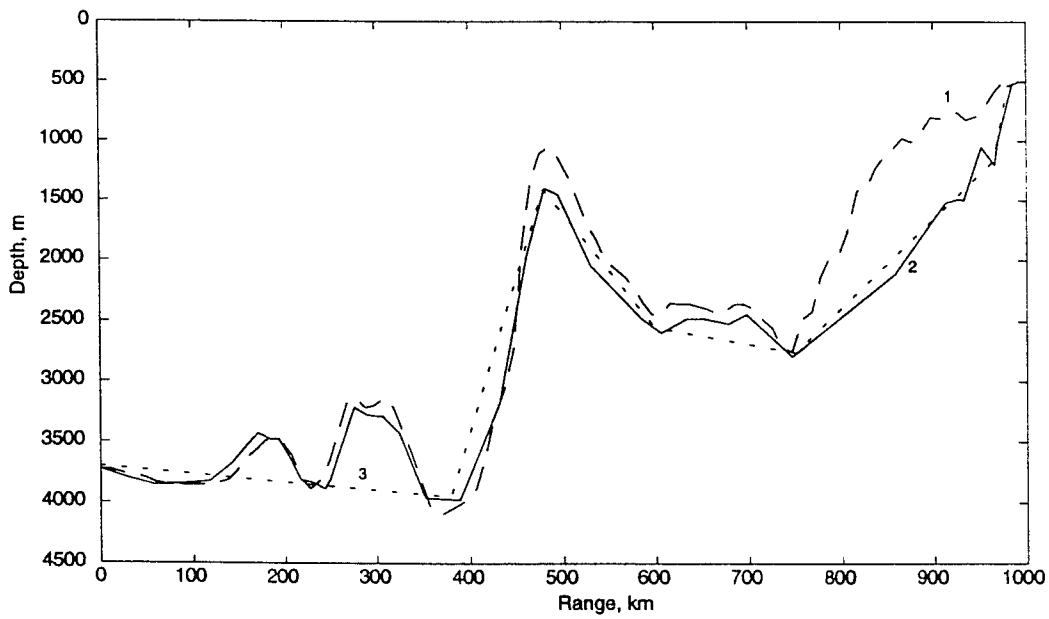

Fig.6. Bottom profile along the path TURPAN-NARWHAL: 1 -according to the 5-minute topographic grid; 2 - according to [6]; 3 - approximation for acoustic modeling

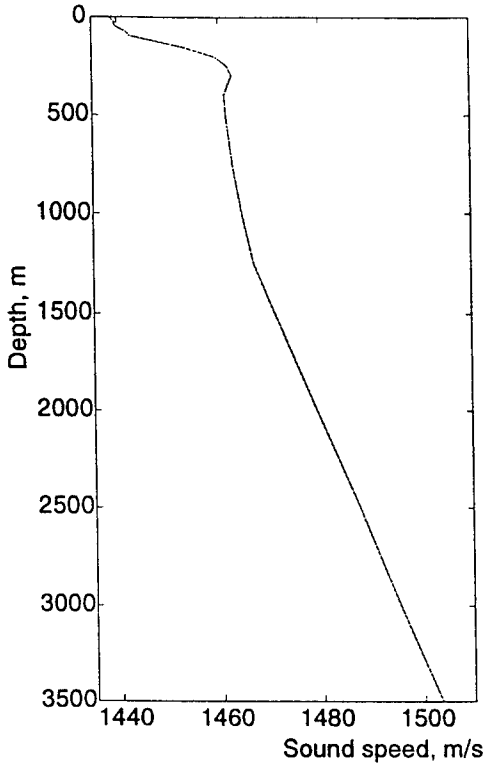

Fig.7. Sound speed profile measured at TURPAN

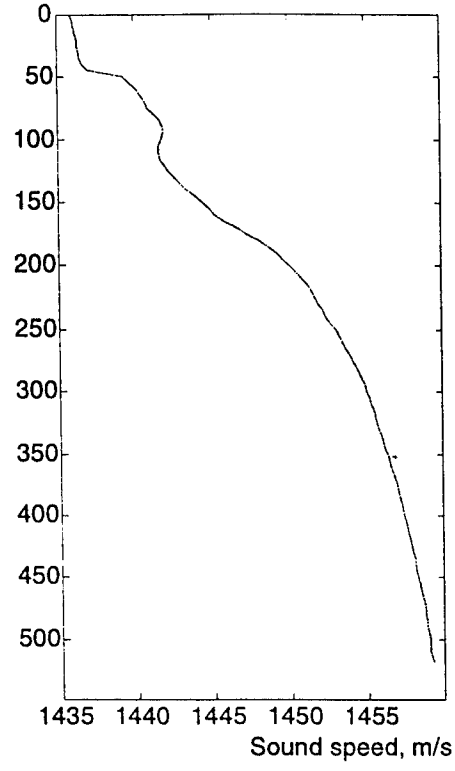

Fig.8. Sound speed profile measured at NARWHAL

Table 1. Log of TURPAN - NARWHAL transmissions

TURPAN						NARWHAL			
N	Day	Time Start/End	Freq, Hz Len/Digit*	Level,dB strt/end	Transmission comments	Gain	AEL avail	Tape	Reception comments. Valid length, min
1	17	9:00Z/10:00	CW, 19.6	195/194.5	**Rubidium clock - on**	3	-	6	Tape 6 - not available
2		11:00/12:00	CW, 19.6	195		3	-	6	Tape 6 - not available
3		13:00/14:00	**M255/25***	195/194		3	-	6	No Record
4		15:00/16:00	CW, 19.6	195/194.5		3	+	7	60'
5		17:00/18:00	**M511/25**	194.5/194		3	+	7	60'
6		19:00/20:00	CW, 19.6	195/194		3	+	7	60'
7		22:00/23:00	CW, 19.6	195/194.5		3	+	-	
8	18	01:00/02:00	CW, 19.6	195/194.5		3	+	-	
9		04:00/05:00	CW, 19.6	195/194.5		2	+	9	60'
10		07:00/08:00	CW, 19.6	195/194.5		3	+	9	60'
11		09:00/10:00	CW, 19.6	195/194.5		3	+	9	41'
		10:33/			**PowerBreak, rub.clock off**		+	-	
		10:45/			**Power on, rub.clock on**		+		
12		11:00/12:00	CW, 19.6	195/194.5		2-3	+	10	60'
13		13:04/14:00	**M255/12.5**	195/194		3	+	10	35'
		14:06/			**PowerBreak, rub.clock off**		+		
	19				**Power on, rub.clock on**		+		
14	19	18:40/19:00	CW, 21.6	189		3	+	12	21.6 Hz - No use
15		19:00/20:00	CW, 19.6	195		3	+	12	No signal record
16		20:40/21:00	CW, 17.6	191		3	+	12	17.6 Hz - No use
17		22:00/23:00	**M255/12.5**	194.5/194		3	+	12	Not a signal record
18	20	01:00/02:00	CW, 19.6	195.5/195		2	+	13	5'
19		04:00/05:00	**M255/12.5**	195.5/194.5	3 phase jumps	2	+	13	60'
20		07:00/08:00	CW,19.6	195.5/195		2	+	13	60
21		09:00/10:00	CW, 19.6	195.5/195		2	+	13	60
22		11:00/12:00	CW, 19.6	195.5/195		2	+-	13	60
23		13:00/14:00	**M255/12.5**	195/194.5			-	-	No record
24		15:00/16:00	CW, 19.6	195/194.5			-	-	No record
25		17:00/17:57	**M511/12.5**	195/194.5	Phase jump. Poor after 42'		-	-	No record
26		19:00/20:00	CW, 19.6	195/194.5		3	-	14	16'
27		22:00/23:00	CW, 19.6	195/194.5	2 short breaks	3-0	-	14	Not a signal record
28	21	01:00/02:00	CW, 19.6	195/194			-	-	No record
29		04:00/05:00	CW, 19.6	195/194		3	-	15	55
30		07:00/08:00	CW, 19.6	194.5/194		3	-	15	60
31		09:00/10:00	**M127/12.5**	194/193.5		3	-	15	30' valid.
32		11:00/12:00	CW, 19.6	194.5/194		3?	-	16	Tape 16 - BAD
33		13:00/14:00	**M1023/12.5**	194/193.5			-	16	Tape 16 - BAD
34		15:00/16:00	CW, 19.6	194/193	Two short breaks at 15'	2-3	-	17	15'
35		17:00/18:00	**M511/12.5**	193.5/193	Wrong sequence law.	3	-	17	Bad, very noisy.
36		19:00/20:00	CW, 19.6	194/193.5		3	-	17	60
37		22:00/23:00	CW, 19.6	194/193		3	-	17	60
38	22	01:00/02:00	CW, 19.6	194/193	2 breaks. Level decrease.	0	-	18	Tape 18 - not available
39		04:00/05:00	CW, 19.6	/193			-	18	Tape 18 - not available
40		07:00/08:00	CW, 19.6	193.5/193			-	18	Tape 18 - not available
41		09:00/10:00	**M127/12.5**	193/192.5			-	18	Tape 18 - not available
42		11:00/12:00	CW, 19.6	193/192.5			-	18	Tape 18 - not available
43		13:00/14:00	**M255/12.5**	193/191.5	Distorted waveform		-	19	Tape 19 - not available

*MXXX/YY- M-sequence length XXX digits, YY periods of carrier per digit.

Additional comments:

1. There were not breaks and phase jumps during transmission, if it is not noted in the table.
2. All phase jumps relate to both digit. This is common phase shift relatively the carrier.
3. The attached files with the phase modulation series contain the actual order of the signal phase that has been obtained after demodulation of the recorded signals and normalization.

Transmitted signals

The acoustic source was deployed at TURPAN at a depth of 60 m. Forty-three CW and broadband acoustic signals, lasting 1 hour each, were transmitted at 19.6 Hz during 5 days of the experiment (see a compete list of the TAP transmissions in Table 1). The broadband signals (bold records in Table 1) were generated via digital modulation of the signal phase by $\pi/2$ synchronised with the pseudorandom Maximal Length Sequences (M-sequences or MLS). The duration of each digit in the M-sequences (pulse width) was either 12.5 or 25 periods of the carrier frequency. The period of the M-sequences was 127, 255 or 511 digits. Such modulation reduces the spectral level of the carrier frequency by 3 dB. The other half of the signal energy is mostly concentrated within the main-lobe of the signal spectrum which has an effective width of about 3 Hz for a pulse width of 12.5 periods, and 1.5 Hz - for 25 periods.

III. PROCESSING OF THE SIGNALS RECEIVED AT NARWHAL

Primary processing

A vertical linear array (VLA) of 20 hydrophones was suspended from the ice at station NARWHAL. Most of the hydrophones in the array were spaced at 30m intervals. The total array length varied slightly during the experiment, being approximately 470 m. The bottom depth at NARWHAL was about 530 m, therefore the array intersected the underwater waveguide almost totally.

The signals received on the VLA were digitised by a 16-bit ADC with a sampling frequency of 256 Hz, and recorded on tapes with an Exebyte drive. Unfortunately, the set of signal records is not complete – some of the records are missing, incomplete or defective (see column 10 in Table 1). Twenty-seven of the total of thirty-five signals recorded at NARWHAL, were provided for us on tapes 7-17. Only 21 of these signal records are suitable for processing. Tapes 6, 18, and 19 with 8 more signals are not still available to us.

The procedure of primary processing of the TAP signals included complex demodulation, low-pass filtering, and resampling with a lower rate. The CW signals were filtered in a passband of ± 0.042 Hz, and downsampled with a rate of 0.1 Hz. The MLS signals were filtered in a passband of ± 3.8 Hz, and resampled at 8 Hz.

Post-processing

Post-processing of the MLS signals included the procedure of pulse compression, i.e. computing correlation of the received signal and the MLS replica, and coherent averaging of the resulting complex pulse-compressed signal by the MLS periods. For coherent averaging, the phase of the MLS signals was preliminarily corrected for the Doppler shift due to relative drift of TURPAN and NARWHAL. The Doppler shift was determined by tracking the variations in the phase of the carrier frequency.

Figure 9 shows the typical arrival pattern (magnitude of the pulse-compressed signal) of the MLS signal received on a single VLA hydrophone at NARWHAL. The last small peak (687 sec) in the pulse form of the signal corresponds to mode 1. The modes of the higher numbers are not separated by the travel time - they arrive almost simultaneously, forming a high pulse, at 680 sec. The arrival pattern of the MLS signals received at NARWHAL, is unlike that of the TAP signals received at SIMI, where, after pulse compression, modes 1-4 were sharply resolved in the time domain [4]. This dissimilarity is due to the difference in the propagation distance from TURPAN to NARWHAL and SIMI - the shorter the propagation distance the less difference in the modal propagation times.

Array calibration

The preamplifiers of the VLA hydrophones were operated in four different modes of gain (0-3) switched over with a step of 6 dB (see column GAIN in Table 1). All the VLA receivers (hydrophones with preamplifiers) had been calibrated beforehand.

Noise

Figure 10 demonstrates the mean noise levels on all the VLA receivers measured at 19.6 Hz (0.085 Hz passband) for half hour periods, followed by the TAP signals. Here the noise level is normalised to a 1 Hz frequency band. In Figure 10 particular curves correspond to different transmissions. The bold curve displays the noise level averaged over all the transmissions. The vertical distribution of the noise level shown in Figure 10, is unusually irregular - the noise level on some of the adjacent hydrophones, spaced at 30 m, differs by 2-3 dB. Despite considerable changes in the mean noise level from one transmission to another, such an irregular distribution remained very consistent in all the transmissions, which could point to possible errors in the calibration of the VLA receivers.

The mean levels of the depth-average noise intensity in the various transmissions are shown in Figure 11. The noise level before transmissions 9 and 26 has an offset of about 6 dB relative to that before the preceding and following transmissions. This, possibly, points to inconsistency in the actual gain mode and the entries in the VLA operation log in some of the periods of reception.

Integral energy flux of the signals

Because of the modal interference and relative drift of the source and the receiving array, the signal level on individual hydrophones of the VLA varied from one transmission to another. When the radiation level of the source is constant, the integral energy flux of the acoustic signals through the cross-section of a waveguide should be the same at different distances from the transmitting site. The vertical array at NARWHAL crosses almost all of the underwater acoustic channel, and overlaps those sections of the modal eigenfunctions which carry more than 90% of the modal power. Therefore, the depth-average level of the signals on the VLA should be almost unvarying with a change in distance. We calculated the depth-average intensity of the CW and MLS TAP signals in the narrow frequency band of 0.085 Hz. Figure 12 demonstrates the results of calculations corrected for small changes in the radiation level (see column 5 in Table 1), and 3 dB difference in the carrier level of the CW and MLS signals. Note the offset of the signal levels in transmissions 9 and 26 is similar to that of the noise level in Figure 11. A more important point concerns an evident increase in the depth-average level of the signals in the whole group of transmissions 18-22. This significant increase is roughly 6 dB similar to the gain switch step, though the noise measurements do not apparently point at a mismatch in the array gain in these transmissions.

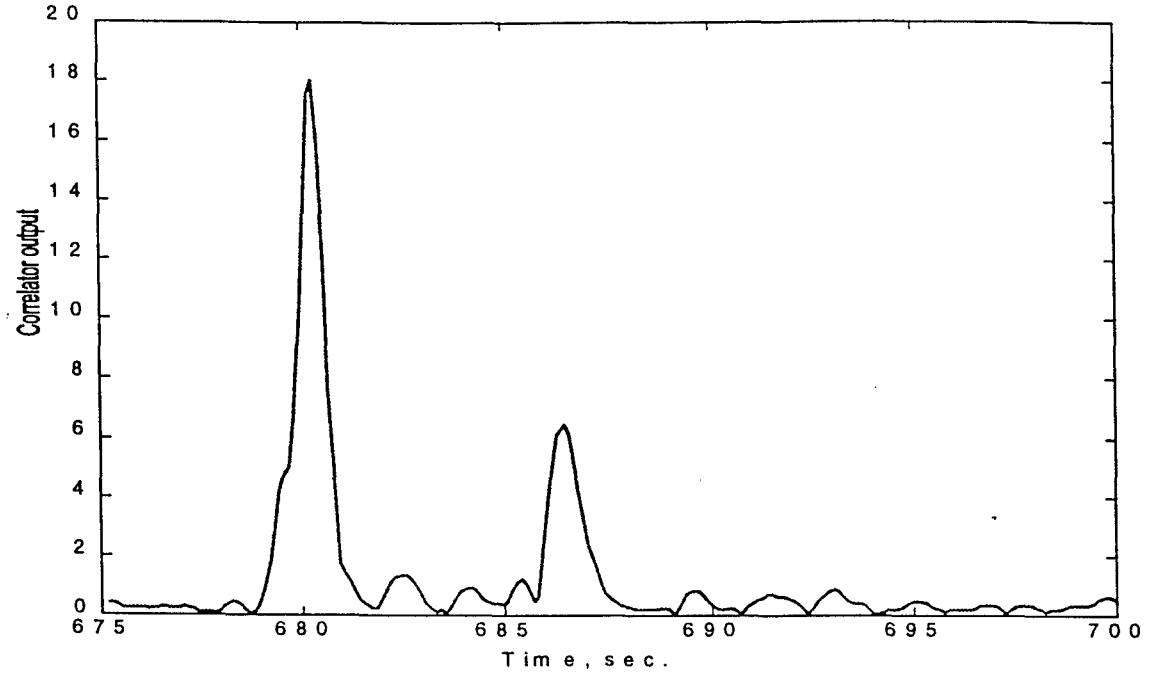

Fig.9. Typical arrival pattern of a pulse-compressed MLS signal at NARWHAL

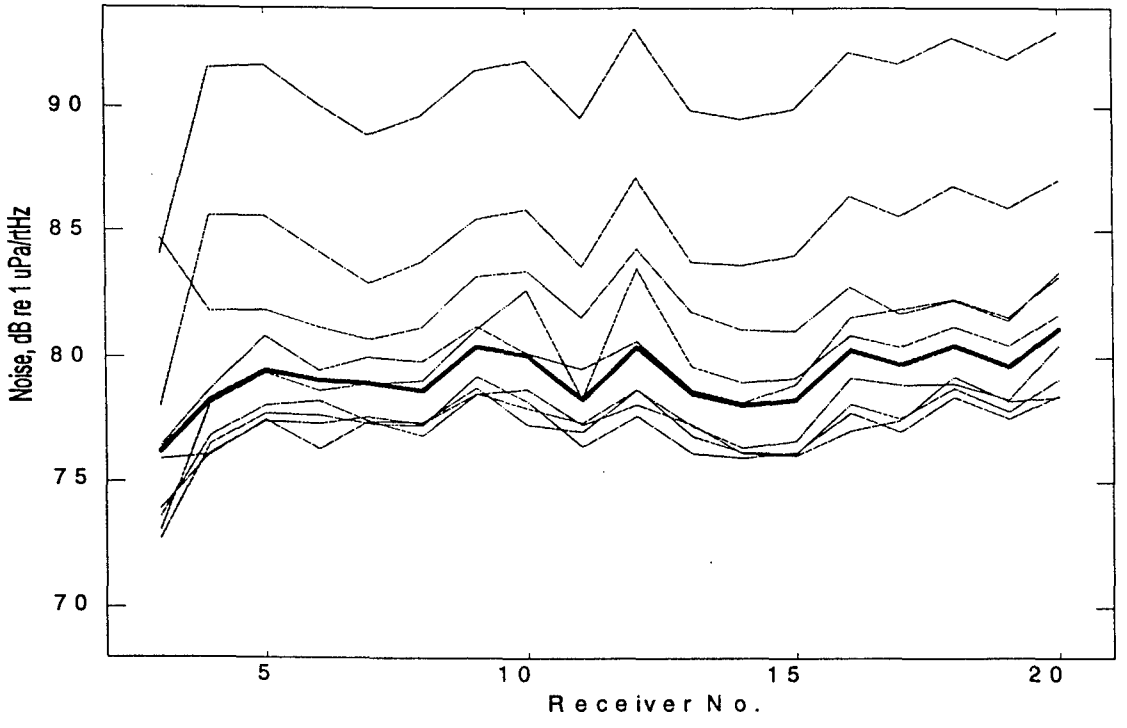

Fig.10. Noise levels on the VLA receivers (some of transmissions 4 - 37)

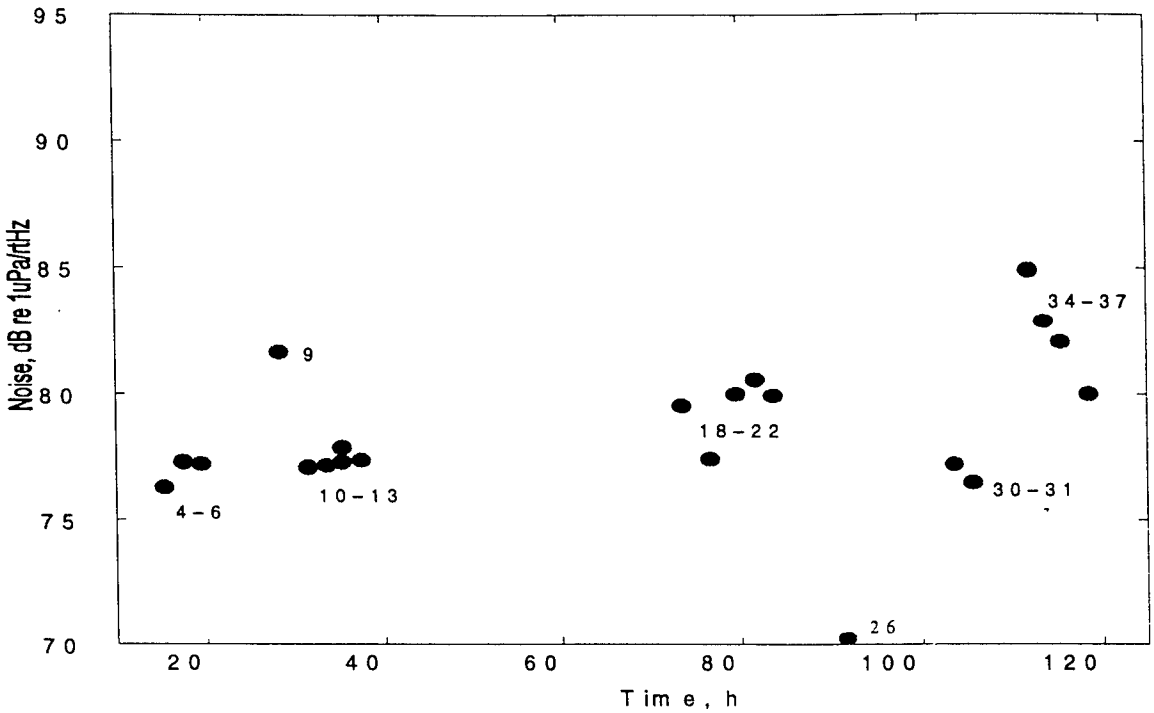

Fig.11. Depth-average intensity of ambient noise

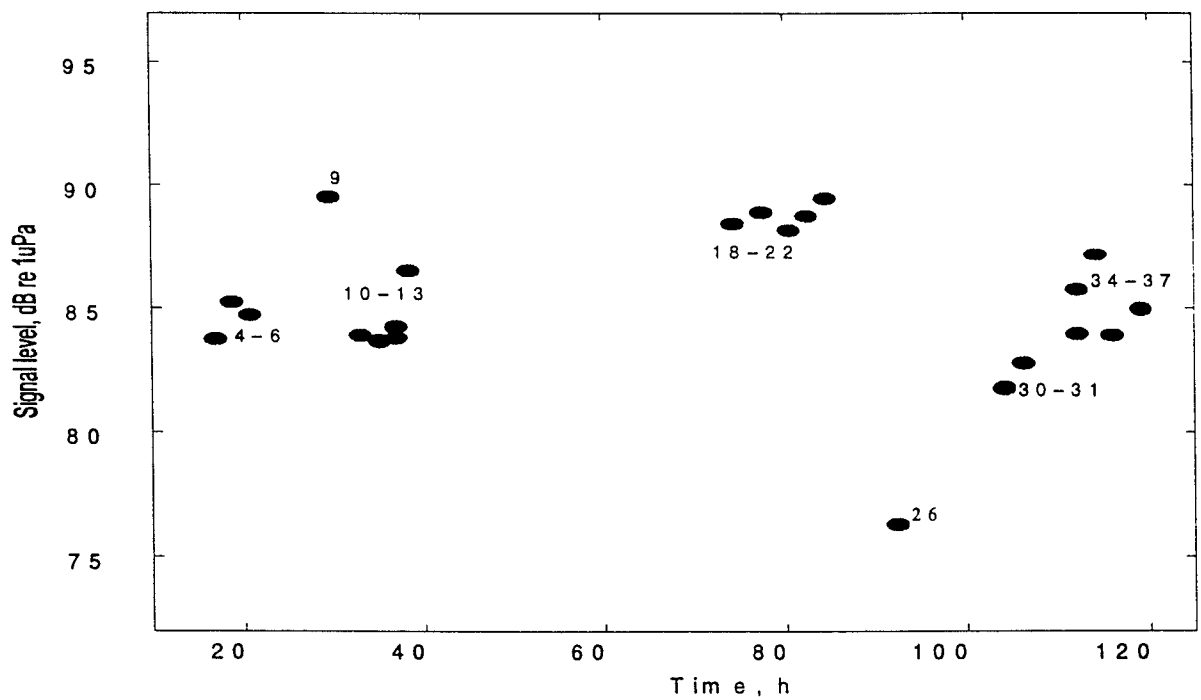

Fig.12. Depth-average intensity of the TAP signals at the carrier frequency

Array Echo-Locating System (AEL)

The VLA was a flexible array suspended from the ice with a weight at the bottom. For tracking changes in the array shape due to variations of the ice drift and the water current, three special receivers were fixed at the midpoint and both ends of the array (33, 282, and 426 m), and four pingers were deployed under the ice at a distance of about 500 m around the array. This echo-locating system provided the data for continuous 3-dimensional location of these three reference points on the array.

For array processing of the TAP signals on the VLA, we calculated the horizontal displacements of the AEL receivers in the direction of the source (48° bearing from NARWHAL to TURPAN). Figure 13 shows the displacements of three AEL sensors along the axis directed to TURPAN during the experiment. Note that the AEL data were available for transmissions 2–22 only. A 24 hour periodicity predominant in the time pattern in Figure 13, indicates the tidal origin of the horizontal motion of the array. The VLA shape in the vertical plane TURPAN-NARWHAL was restored via linear approximation of the horizontal displacements of the hydrophones between the AEL receivers. Figure 14 demonstrates the particular patterns of the array shape recovered from the AEL data. Two extreme curves demonstrate the greatest inclination of the VLA observed. Three other curves show the VLA shape for MLS transmissions 5 and 19. Two curves related to transmission 19 demonstrate significant change in the VLA inclination from the beginning to the end of a 1 hour period.

Correction of the array shape for signal processing

Spatial filtering of the acoustic modes (considered below) requires correction of the signal phase on the VLA hydrophones for compensation of the horizontal inclination of the array. We used the AEL data for phase correction. The validity of phase correction was verified from the vertical phase distribution of mode 1 which should be, theoretically, uniform. It was possible because this mode in the MLS signals was separated in time from other modes. Figures 15, 16, and 17 demonstrate the phase of mode 1 versus the depth of the VLA hydrophones in signals 5, 13 and 19 respectively, before and after correction for the AEL data. The effect of phase correction is evident for transmission 19 – the AEL-corrected phase of mode 1 is close to uniform. In two other transmissions, the VLA hung almost vertically (see Figure 13), therefore the AEL correction did not yield noticeable results. Note that phase compensation based on the AEL data does not completely correct the phase of mode 1, particularly on the deep hydrophones. This is, possibly, due to a low SNR of mode 1. The amplitude of mode 1 falls rapidly with depth below 200 m (see Figure 18), which leads to a considerable decrease in the SNR and substantial errors in the phase measurements.

In the transmissions ignored for the AEL data, the temporal separation of mode 1 in the MLS signals allowed us to estimate, approximately, the array inclination directed to the source, from the vertical profile of the modal phase on the VLA. Figure 19 shows the phase profile of mode 1 on the VLA in transmission 31 which was not provided with the AEL data. In the case shown, the phase profile is close to uniform (except for the deepest hydrophone), which indicates a somewhat vertical position of the VLA.

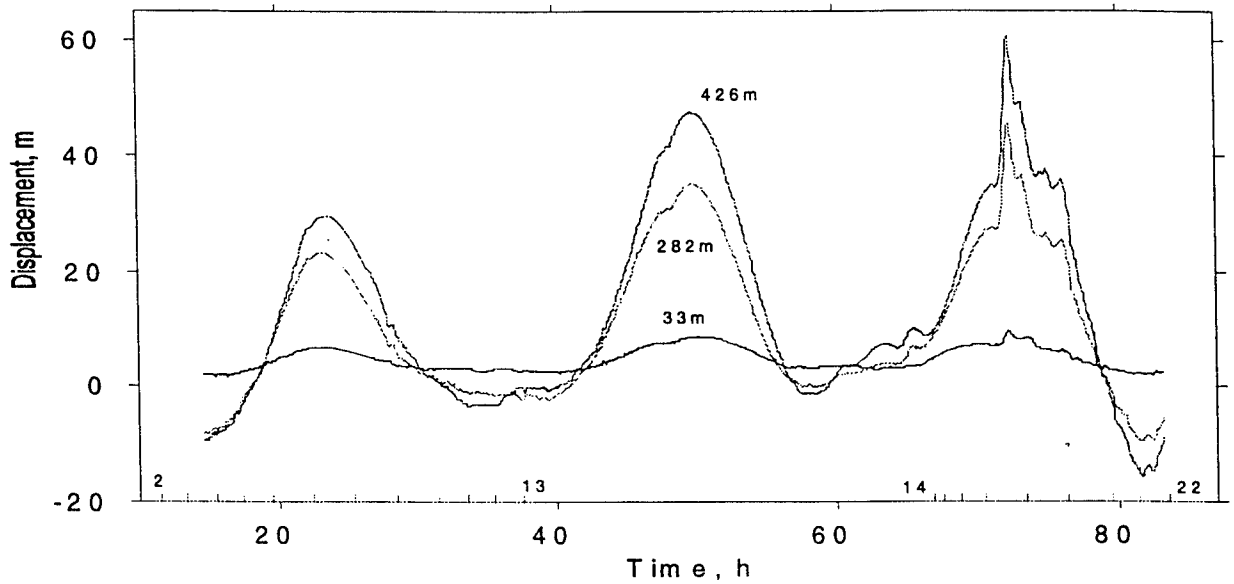

Fig.13. Displacement of the AEL receivers on the VLA (depth 33 m, 282 m, and 426 m) in the direction from TURPAN to NARWHAL

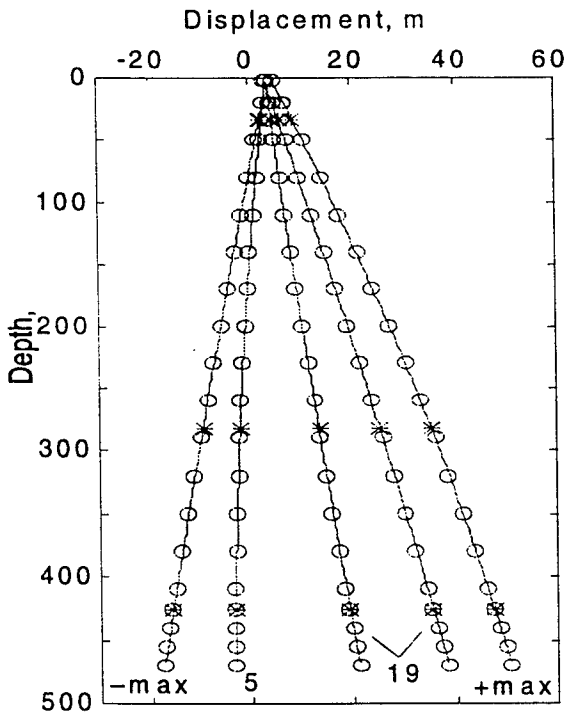

Fig.14. Shape of the VLA in the vertical plane TURPAN-NARWHAL restored from the AEL data (transmissions 5 and 19, and the extreme inclination)

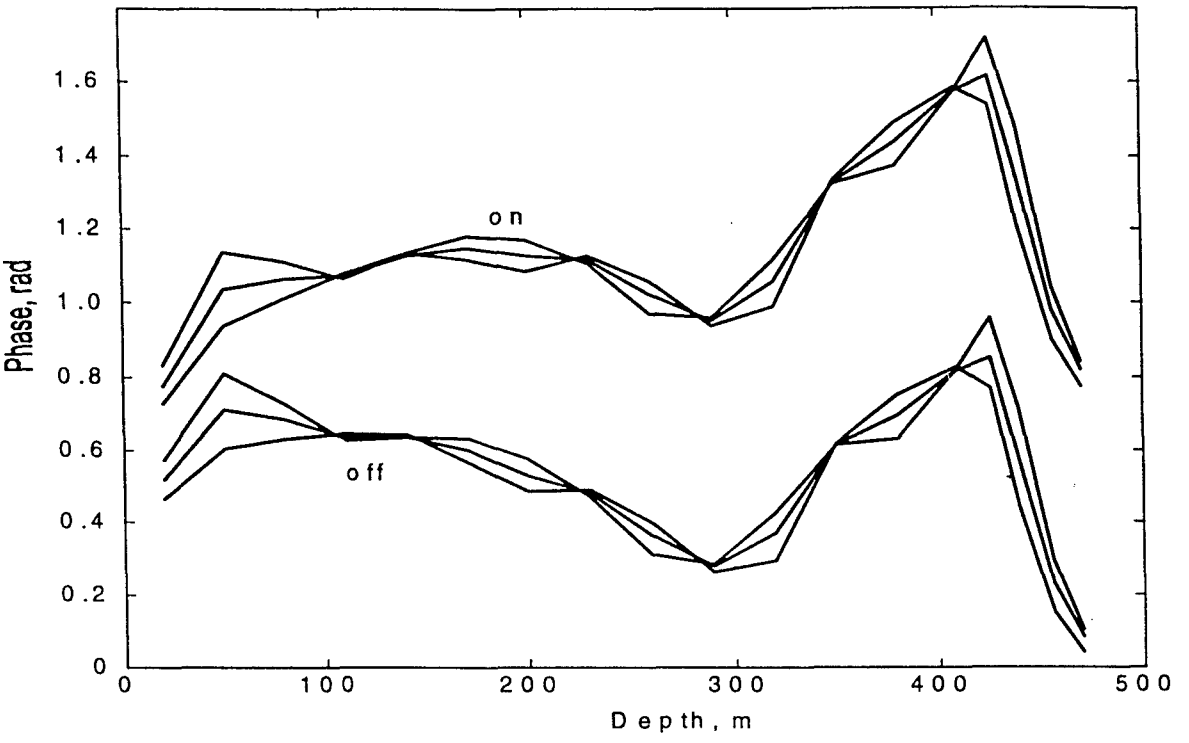

Fig.15. Vertical phase profile in mode 1 (start/mid/end of transmission 5): "off" - before AEL compensation of phase, "on" - after AEL compensation

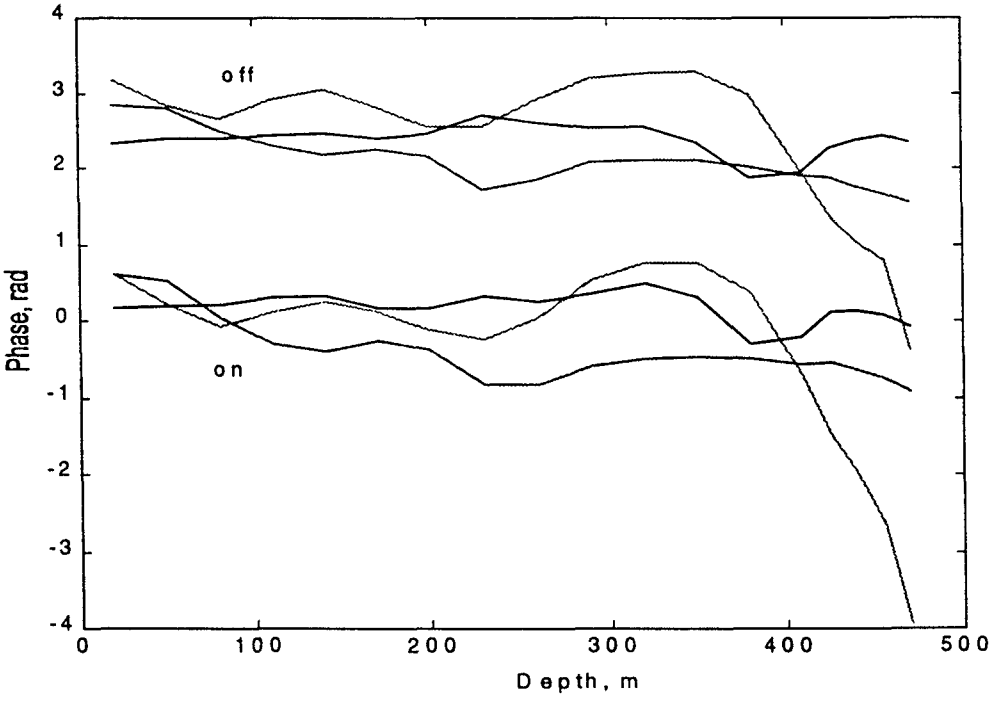

Fig.16. Vertical phase profile in mode 1 (start/mid/end of transmission 13): "off" - before AEL compensation of phase, "on" - after AEL compensation

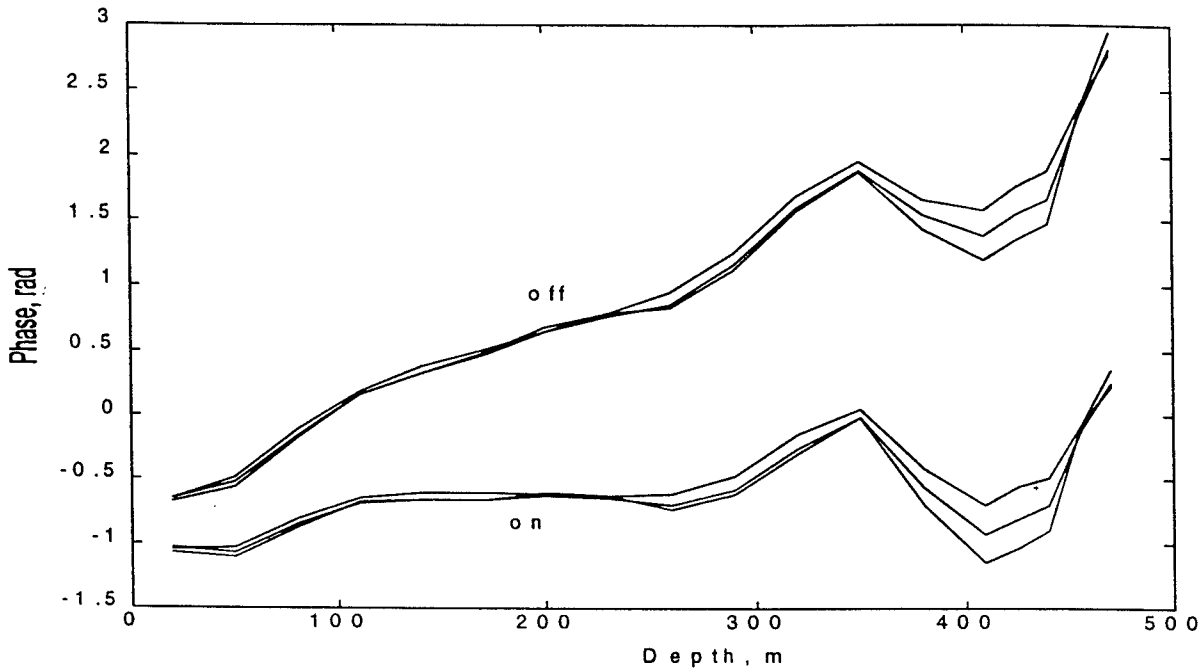

Fig.17. Vertical phase profile in mode 1 (start/mid/end of transmission 19): "off" - before AEL compensation of phase, "on" - after AEL compensation

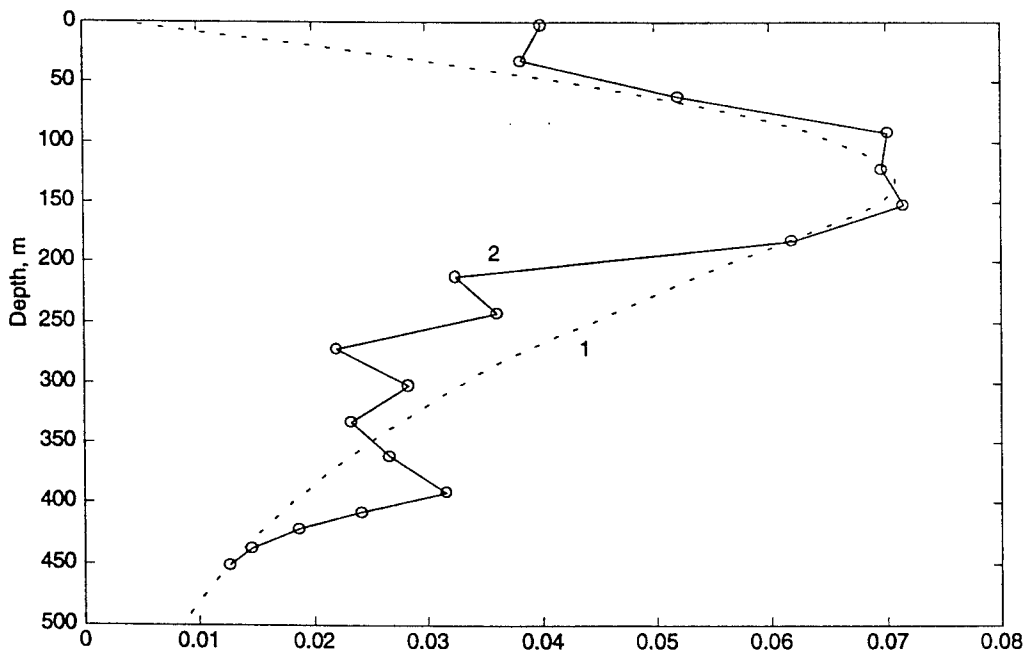

Fig.18. Vertical profile of mode1: 1 - computed, 2 - measured in the MLS signal (transmission 19)

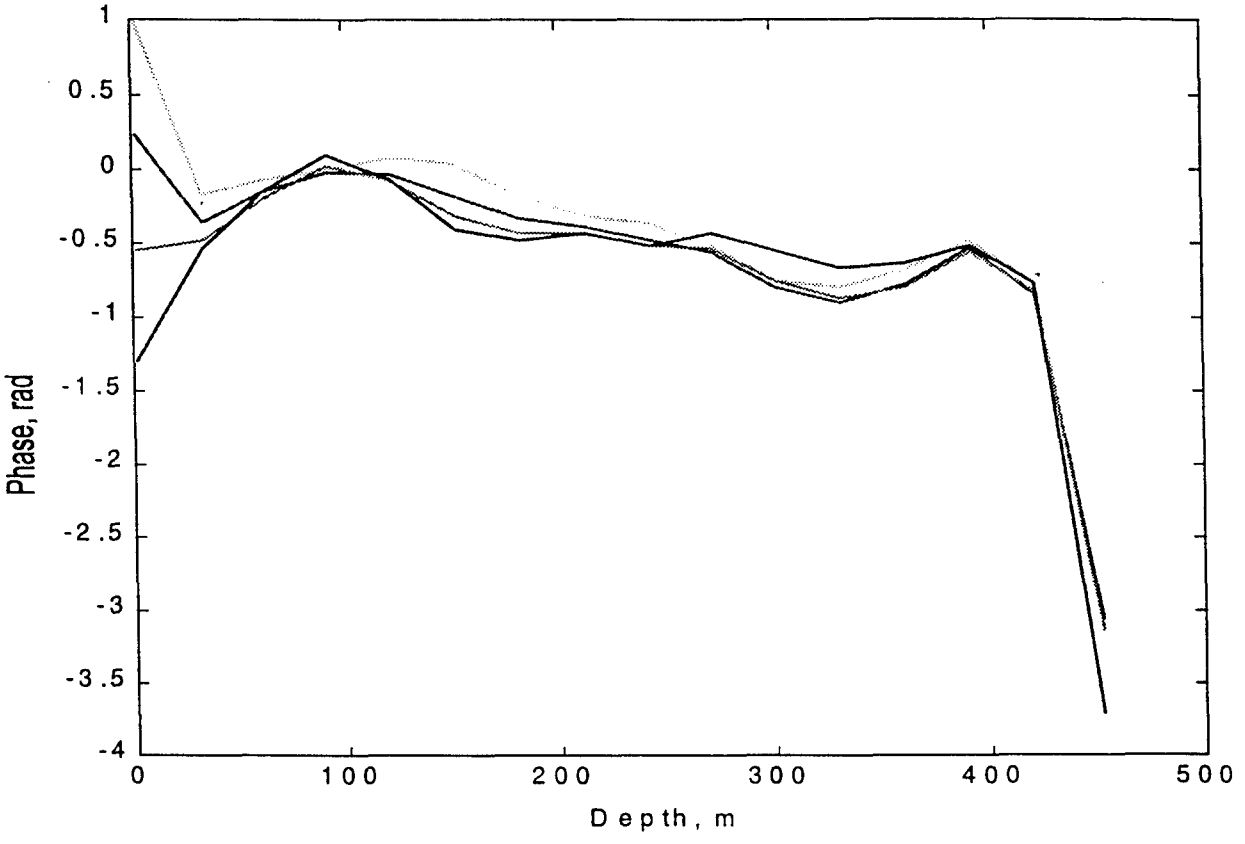

Fig.19. Vertical phase profile in mode 1 (start/mid/end of transmission 31) without AEL compensation

Mode filtering

In the TAP signals received at NARWAL, the modes of numbers higher than 1 were not resolved in time. Therefore, we used spatial filtering of those modes on the vertical array. We applied the Least Mean Square (LMS) estimation method for resolving the complex modal amplitudes. The sound field on the VLA hydrophones can be represented in matrix form as

$$\mathbf{P} = \mathbf{FA},$$

where **P** is a column-vector of complex sound amplitudes at the horizons of the VLA hydrophones, **F** is the matrix of modal eigenfunctions on the VLA hydrophones, and **A** is the column-vector of the complex modal amplitudes. The LMS estimation implies minimization of the measure

$$\left|\tilde{\mathbf{P}} - \mathbf{P}\right|^2, \qquad (1)$$

where $\tilde{\mathbf{P}}$ is the vector of the complex amplitudes of the signals received on the VLA hydrophones. Minimization of (1) leads to the following system of linear equations with respect to the modal amplitudes **A**:

$$\mathbf{A}(\mathbf{F}'\mathbf{F}) = \left(\mathbf{F}'\tilde{\mathbf{P}}\right)' \qquad (2)$$

The solution of (2) is

$$\mathbf{A} = (\mathbf{F}'\mathbf{F})^{-1}\left(\mathbf{F}'\tilde{\mathbf{P}}\right)' \qquad (3)$$

When the span of a vertical array does not completely overlap the modal eigenfunctions, the LMS estimates (3) of the modal amplitudes are more correct and more constant with respect to the relative phase of the modes, than the traditional method of modal decomposition based on a simple formula: $\mathbf{A} = \left(\mathbf{F}'\tilde{\mathbf{P}}\right)'$ (here $\mathbf{F}'\mathbf{F}$ is assumed to be an identity matrix, because of a mutual orthogonality of the eigenfunctions). Note that the LMS estimation is valid, if the number of hydrophones exceeds the actual number of modes making up the sound field. As shown below, the number of significant modes in the TAP signals received at NARWHAL should not exceed 8. If the eigenfunctions presumed for modal filtering correspond to the real eigenfunctions at the receiving site, and the array inclination is negligibly small or completely compensated, then the error of estimates for the modal amplitudes $\tilde{\mathbf{A}}$ follows from formula:

$$\mathrm{Var}\left\{\left[\tilde{\mathbf{A}} - \mathbf{A}\right]^2\right\} = (\mathbf{F}'\mathbf{F})^{-1}\left[(\mathbf{F}'\mathbf{F})^{-1}\right]'(\mathbf{F}'\mathbf{N}\mathbf{F}), \qquad (4)$$

where **N** is the covariance matrix of noise on the vertical array.

To calculate the eigenfunctions of the waveguide at the receiving site, we used the sound speed profile measured at NARWHAL, and the acoustic characteristics of the bottom sediments in the Lincoln Sea given in [2]. A multi-layer structure of the bottom sediments was approximated by a simplified two-layer model with the parameters shown in Table 2.

Table 2. The acoustic model of the bottom in the Lincoln Sea

Layer No.	Depth	Density	Compr. wave speed	Compr. wave attenuation	Shear wave speed	Shear wave attenuation
1	0-30 m	2.15	1770 m/s	0.04 dB/m/kHz	200 m/s	15 dB/m/kHz
2	below 30 m	2.2	1850 m/s	0.2 dB/m/kHz	350 m/s	16 dB/m/kHz

Consider the results of mode filtering. Figures 20-23 show the signal form of modes 1-5 after spatial filtering in transmissions 5, 13, 19, and 31 respectively (the only MLS transmissions available for complete processing). In these plots the amplitude is scaled in $\mu Pa \cdot m^{1/2}$, since the eigenfunctions are normalized over depth. Note the significant difference between the modal amplitudes in transmission 19 and the three other transmissions. This difference is approximately the same (5-7 dB) as in the depth-average intensity of the carrier (Figure 12). The pulse amplitudes of modes 1-8 measured in the transmissions mentioned are jointly shown in Figure 24. Here the signal amplitude in transmission 19 is corrected for -6 dB.

IV. MODAL PROPAGATION LOSS

Experimental results

Figure 24 demonstrates the propagation loss (PL) of modes 1-8 corrected for the modal excitation coefficients and cylindrical spreading, i.e. :

$$PL_m = RL - 20\text{Log}Z_m(z_0) - 10\text{Log}(R) - 20\text{Log}A_m \qquad (4)$$

where RL is the acoustic radiation level of the source (see Table 1), $Z_m(z)$ are the modal eigenfunctions at the transmitting site, $z_0 = 60$ m - the depth of the source, R is the propagation distance (in meters), and A_m the measured modal amplitudes. In the adiabatic approximation the modal propagation loss can be expressed through the modal attenuation coefficients $\alpha_m(r)$ as follows:

$$PL_m = \int_0^R \alpha_m(r)dr .$$

For comparison, the propagation loss of modes 1-4 in the TAP signals received at SIMI, has been represented in the same way (4), and also shown in Figure 24. Taking into account the difference in the distances from TURPAN to NARWHAL and SIMI, one can conclude that the range-average modal attenuation coefficients at the TURPAN-NARWHAL path is considerably higher than those at the TURPAN-SIMI path.

Comparison with the modeling results

To model the signal propagation from TURPAN to SIMI, we used a coupled-mode method of calculation of the sound field in the Arctic waveguide [5, 6], because the bottom relief along the propagation path has significant slopes midway (the Morris Jessup Ridge), and, especially, at the end of the path (Canadian continental slope). We assumed that the bottom profile (3) in Figure 6 characterizes the bathymetry in the Lincoln Sea more realistically than the 5-minute bathymetry data. All the results of modeling for the modal propagation loss presented below, have been obtained for a CW signal of 19.6 Hz.

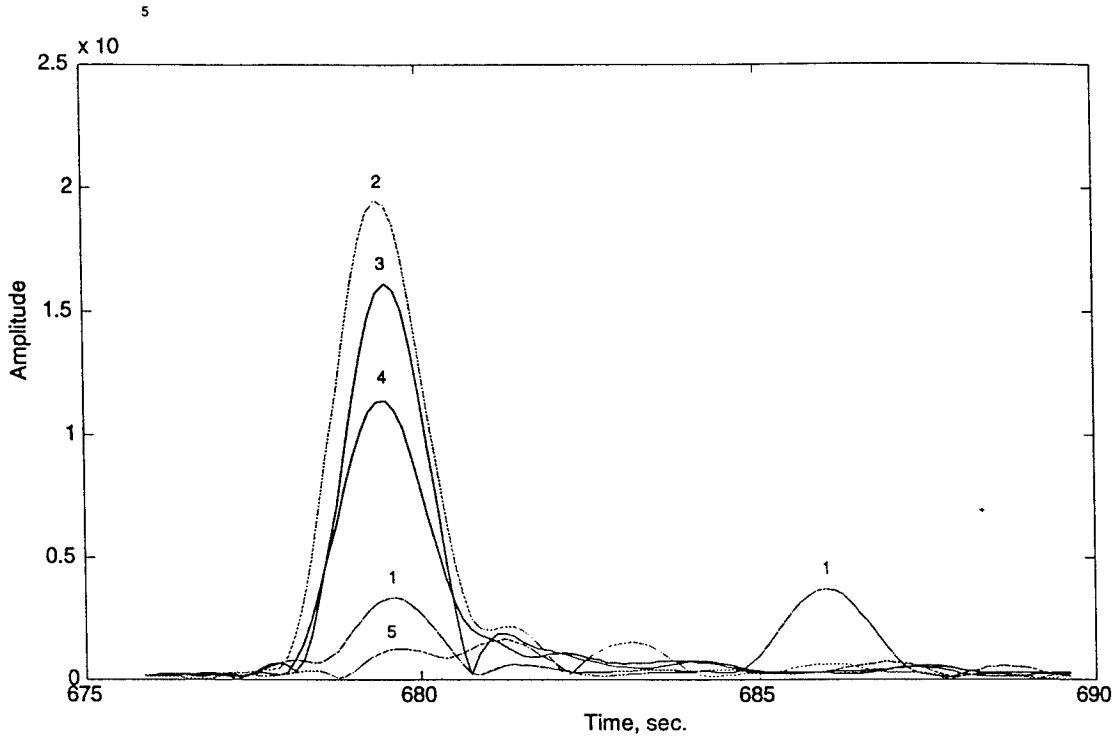

Fig.20. Signal form of modes 1-5 after pulse compression and spatial filtering on the VLA (transmission 5).

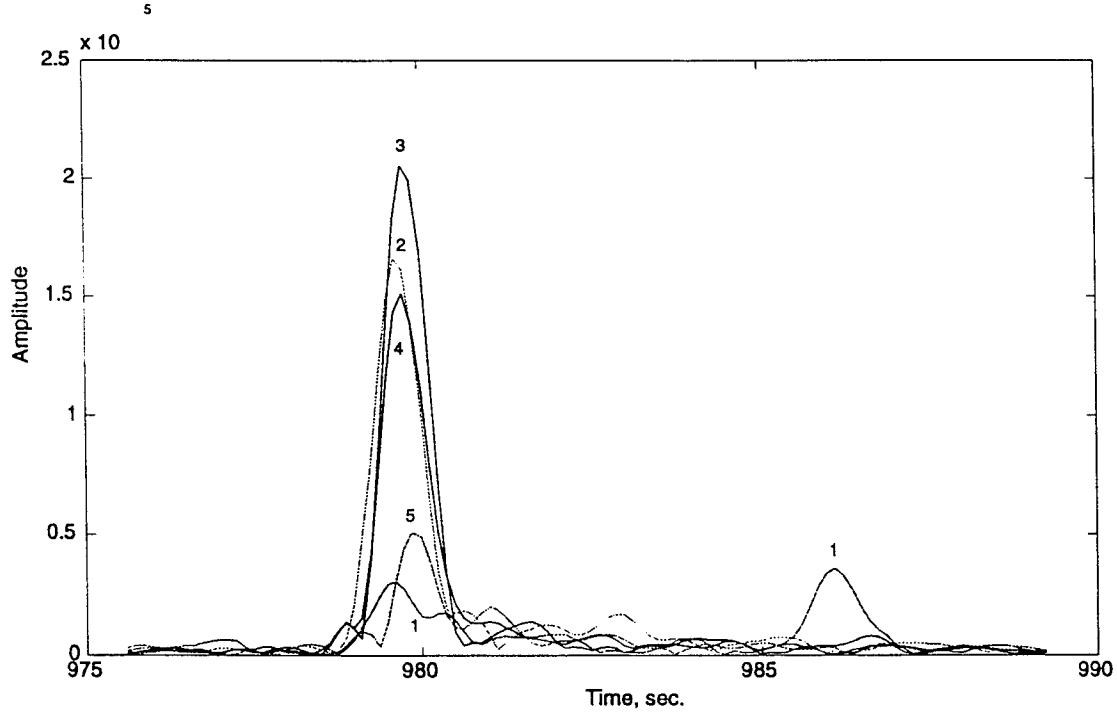

Fig.21. Signal form of modes 1-5 after pulse compression and spatial filtering on the VLA (transmission 13, start delayed).

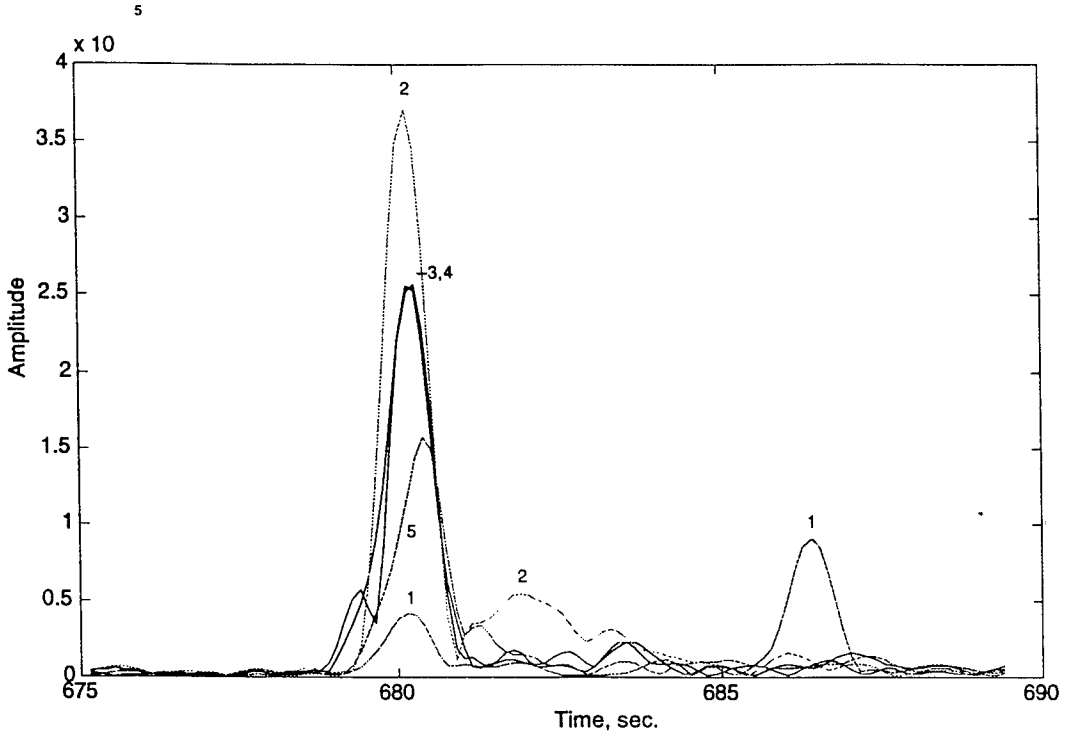

Fig.22. Signal form of modes 1-5 after pulse compression and spatial filtering on the VLA (transmission 19)

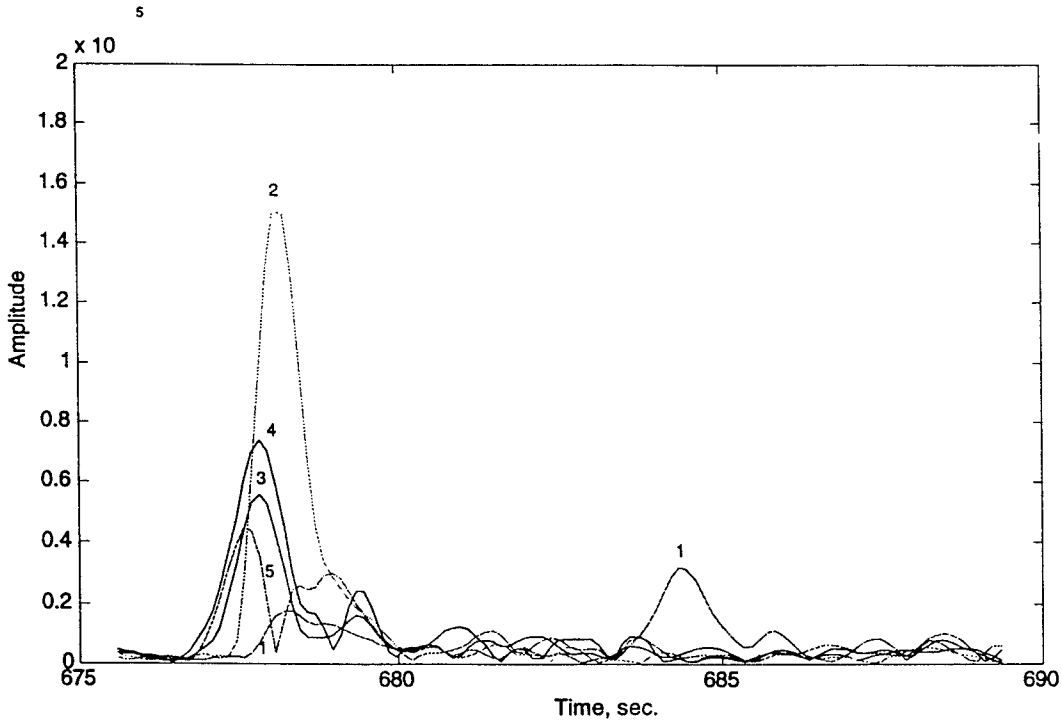

Fig.23. Signal form of modes 1-5 after pulse compression and spatial filtering on the VLA (transmission 31)

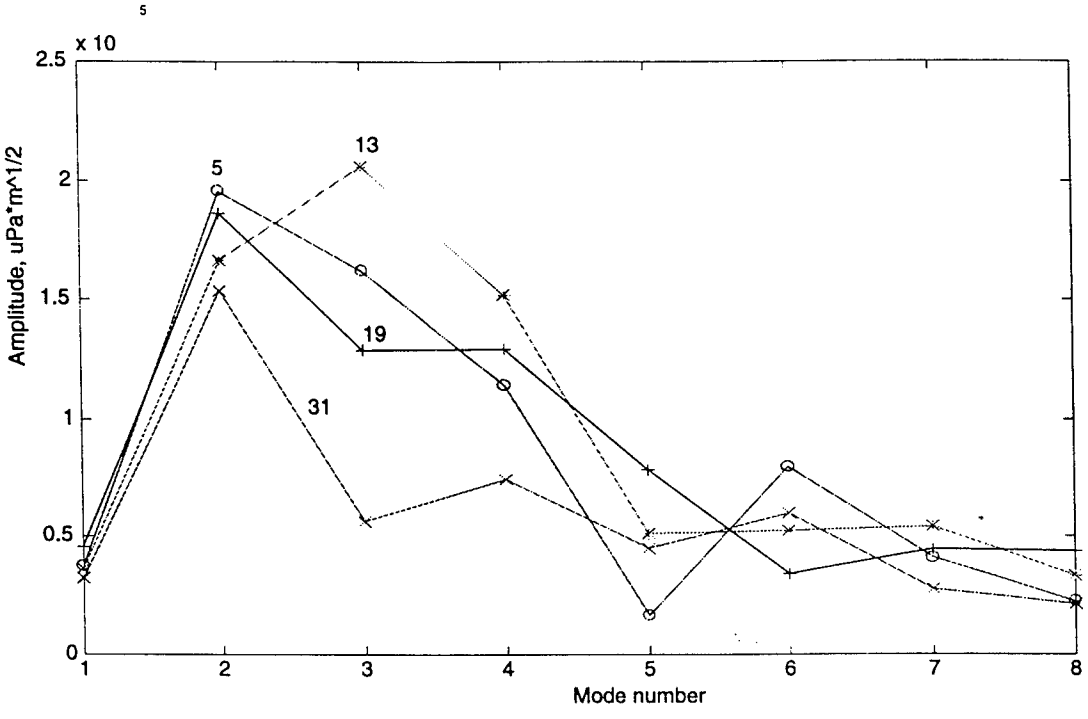

Fig.24. Modal amplitudes in transmissions 5, 13, 19, and 31 (here level of signal 19 is corrected for -6 dB)

In the waveguide model, the whole of the TURPAN-NARWHAL path was separated into 6 sections: the deep-water Eurasia Basin, the eastern slope of the Morris Jessup Ridge, the western slope of the Morris Jessup Ridge, the deep-water region north of the Lincoln Sea, the steep Canadian continental slope, and the continental shelf in the Lincoln Sea. The bottom profile within each section was estimated linearly. The sound speed profiles were set at the beginning and the end of each section, and interpolated linearly within the sections. For the beginning and the end of the path, we used the real sound speed profiles measured at TURPAN and NARWHAL, while other profiles were taken from the POLEX data base. The physical characteristics of the ice were assumed to be uniform along the whole path. They are as follows: density - 0.9, compressional wave speed (real(C_l)) - 3000 m/s, shear wave speed (real(C_s)) - 1800 m/s, compressional wave attenuation (imag(C_l)/real(C_l)) - 0.01. shear wave attenuation - 0.035. The ice statistics parameters were assumed to be constant within each section. They were chosen for modeling as shown in Table 3.

Table 3. Ice statistics parameters along the path TURPAN-NARWHAL assumed for acoustic modeling (STD - roughness standard deviation)

Section No.	Distance [km]	Mean ice thickness, [m]	STD of lower boundary, [m]	STD of upper boundary, [m]	Correlation length, [m]
1	380	4	2.7	0.7	40
2	100	4	2.7	0.7	40
3	120	5	3.3	0.8	40
4	150	5.5	3.6	0.8	40
5	215	6	4	1.0	35
6	15	6.5	4.3	1.1	35
7	11	6.5	4.3	1.1	35

The mean ice thickness and the standard deviation of the lower ice boundary shown in Table 3, coincide in general with contour mapping of the ice statistics parameters in the Arctic Ocean proposed in [7].

The acoustic properties of the bottom sediments along the propagation path were assumed to be the same as in the Lincoln Sea (see Table 2).

Attenuation of the energy flux of modes 1-5 calculated over the TURPAN-NARWHAL path, is shown in Figure 25 (here the energy loss is compensated for cylindrical spreading). This plot clearly demonstrates the difference in attenuation of mode 1 trapped in the upper sound channel, and other modes. The plot also shows an evident increase in the modal attenuation due to growth of the ice thickness and roughness. The Morris Jessup Ridge affects the energy flux of mode 5 (and higher), while mode 1-4 do not noticeably interact with the bottom in this region. The Canadian continental slope influences all the modes, excepting mode 1. There the rapid shallowing of the bottom relief leads to strong modal coupling, which results in considerable oscillations of the modal amplitudes along the propagation path.

In Figures 26, 27 and 28 the modal amplitudes computed with the acoustic propagation model are compared with those measured in the TAP signals in transmissions 5, 19, and 31, respectively. Both the absolute level of the modal amplitudes and the distribution of the signal energy, over different modes, are generally similar in the modeling and experimental results. However, one can notice strong fluctuations in

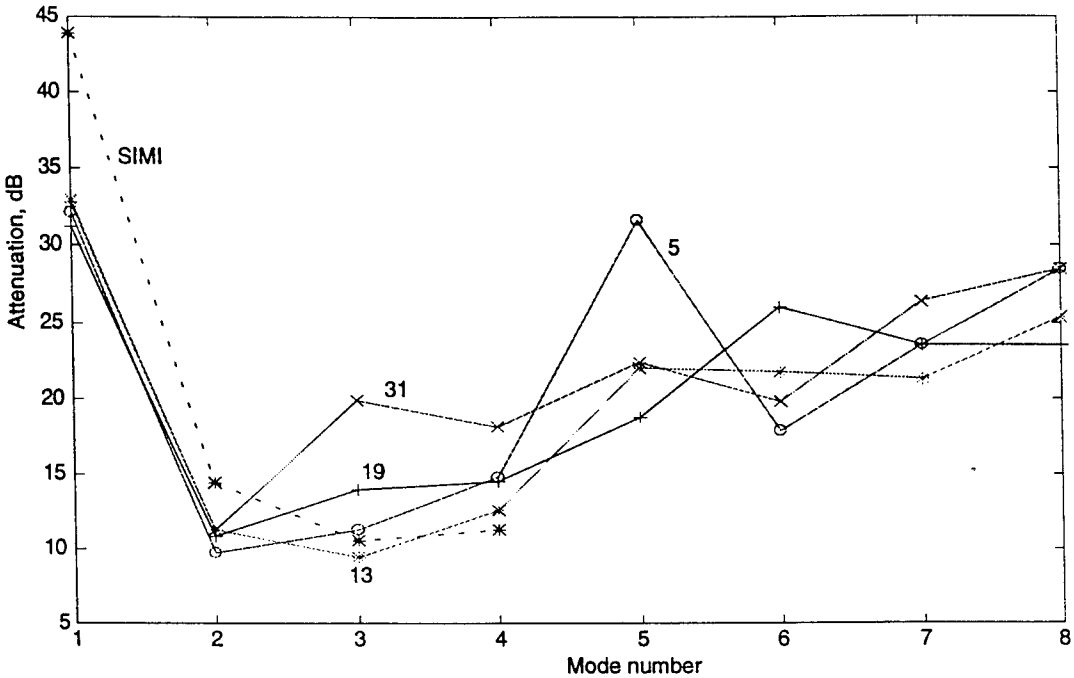

Fig.25. Modal propagation loss corrected for excitation loss and cylindrical spreading (transmissions 5, 13, 19, and 31, and the SIMI data averaged over all the MLS transmissions)

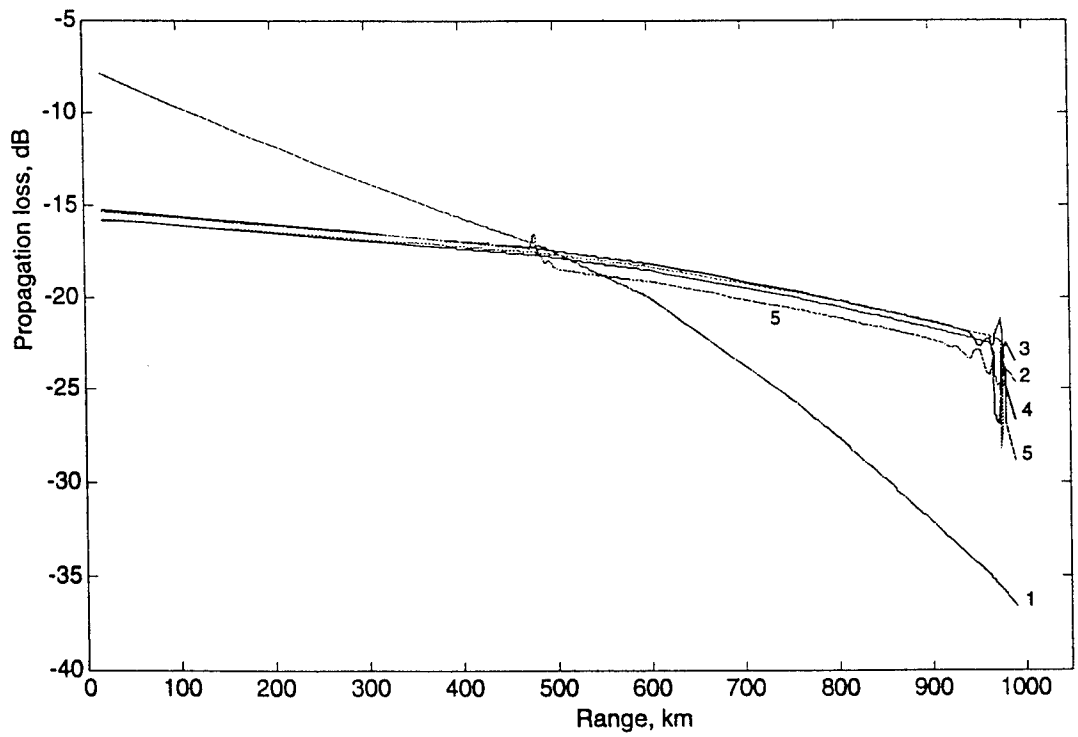

Fig.26. Attenuation of the modal energy flux computed for the path TURPAN-NARWHAL and corrected for cylindrical spreading (modes 1 - 5)

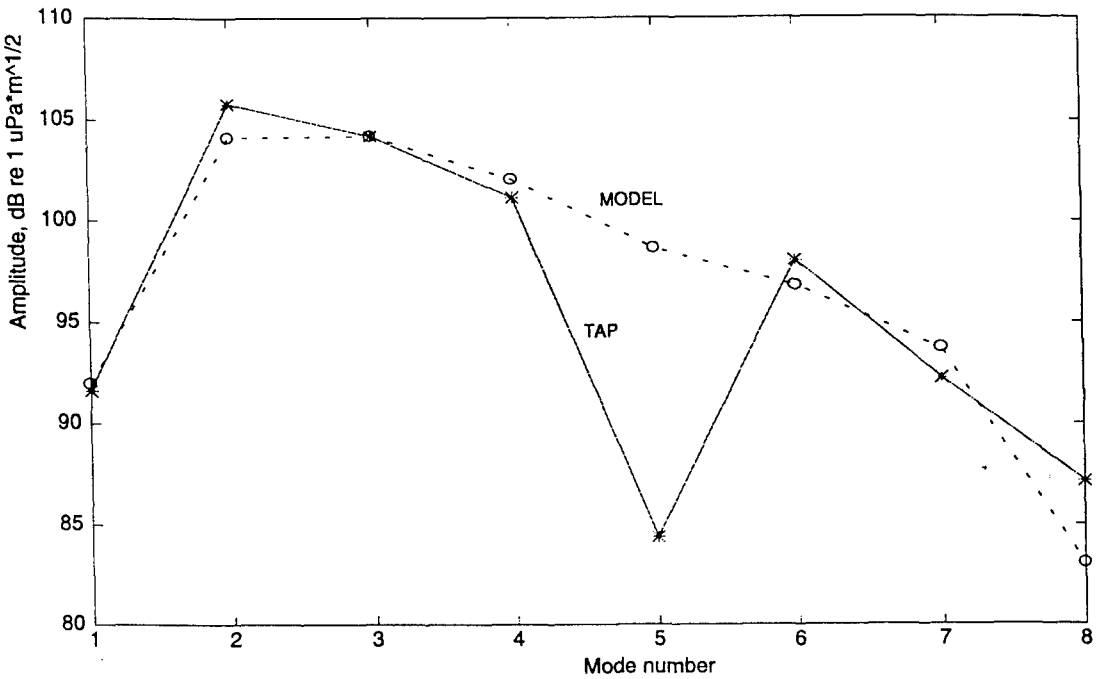

Fig.27. Comparison of the modal amplitudes measured in transmission 5 and computed for the distance of 991.8 km

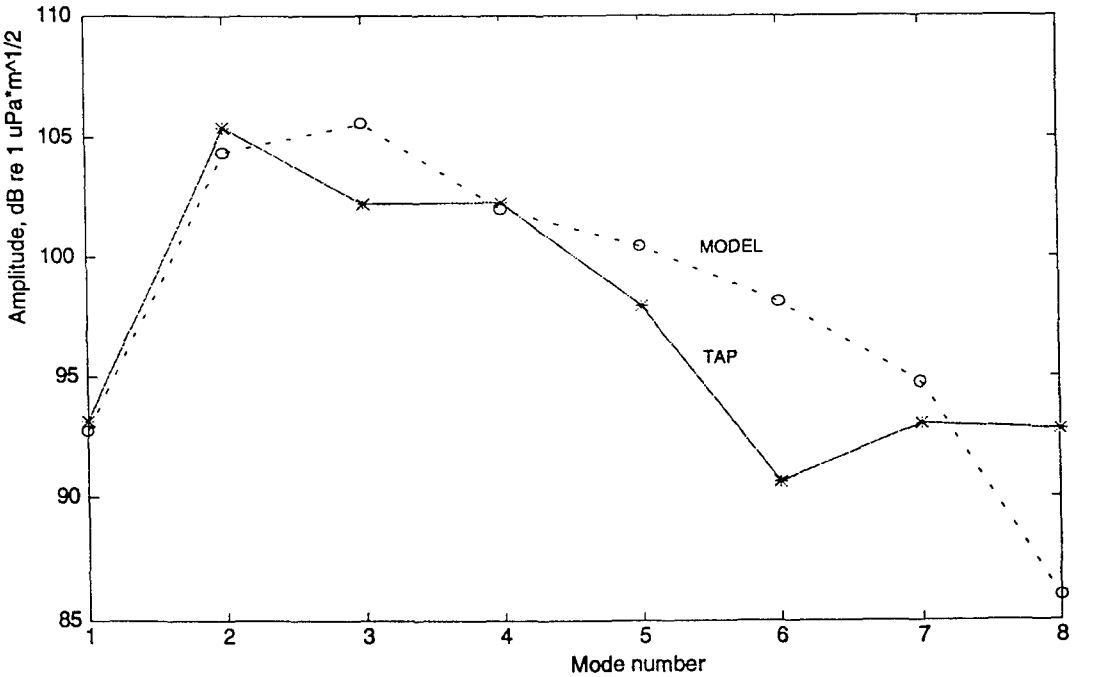

Fig.28. Comparison of the modal amplitudes measured in transmission 19 and computed for the distance of 990.87 km

the modal distribution measured at different distances from the source. Moreover, the theoretical patterns of the modal distribution also show considerable fluctuations. The variations in the experimental results could be related to changes in the bathymetry along the propagation path due to the drift of NARWHAL and TURPAN. As for the theoretical results, such fluctuations seem, at first view, to be surprising. When modeling, we varied only the position of the source, which did not modify the bottom profile along the propagation path. Nevertheless, the modal amplitudes are subject to considerable influence of small variations in the propagation distance, and to the sound speed as well. The explanation of such fluctuations becomes evident after considering the physics of modal coupling. At each cross-section of an irregular waveguide, the intermodal transfer of the acoustic energy flux depends on the vertical distribution of the integral sound field made up of different modes with different phases. Therefore, the effect of modal coupling depends on the relative modal phase. Thus, any changes in the waveguide, even in its regular (horizontally homogenous) parts, leads to changes in the scenario of modal coupling over those sections with irregular parameters. A similar effect has been considered in [8] for ray coupling in a frontal zone.

The results of modal coupling in a variable waveguide are demonstrated in Figure 29, which shows the attenuation of modes 2-5 calculated for three slightly different propagation conditions. The upper plot in this figure is a section of Figure 25 expanded to show the farthest 100 km part of the propagation path in more detail. The middle plot displays the modal attenuation over the same waveguide section calculated for similar sound speed distribution along the propagation path, but with the source placed nearer to the receiving site by 5 km. In the third case (bottom plot), the sound speed in the Atlantic water core (300-500 m) has been decreased by 0.5 m/s on average over a 200 km section of the waveguide (400-600 km range). The comparison of the plots in Figure 29 clearly demonstrates how transformation of modal coupling due to changes in the propagation conditions, leads to strong variations of the modal amplitudes in a CW signal at the receiving site.

V. MODAL TRAVEL TIMES

The travel times of modes 1-5, measured and calculated for transmissions 5, 19, and 31, are given in Table 4. The theoretical travel times were computed in the adiabatic approximation for the sound propagation at 19.6 Hz. One can observe a variable, but always positive difference in the modeling and experimental travel times, most notably in transmission 5. Such a difference is, apparently, the result of the manual control for starting the MLS transmissions at TURPAN. However the modal travel times measured at SIMI should contain the same errors. Table 5 shows the difference in the measured and modeled travel times of modes 1-4 in the signals received at NARWHAL at SIMI.

The values given in Table 5, do not show an evident correlation of the NARWHAL and SIMI data. One can observe only an obvious increase of the difference in the modeled/measured travel times in transmission 5 for both receiving sites. The absence of an evident correlation for these data is not surprising. On the one hand, modes 1 and 2 are affected by strong spatial and temporal variations of the temperature in the upper ocean layers (upper mixed layer and the Atlantic water core). These variations cannot be adequately determined in all details in the acoustic propagation model. On the other hand, the travel time of modes 3 and 4 at the path TURPAN-NARWHAL are very sensitive to changes in the bottom profile over the Canadian continental slope. The approximate bottom profile used in the model, may differ from the real bathymetry of the Lincoln Sea, which could lead to some disagreement of the modeled and measured travel times.

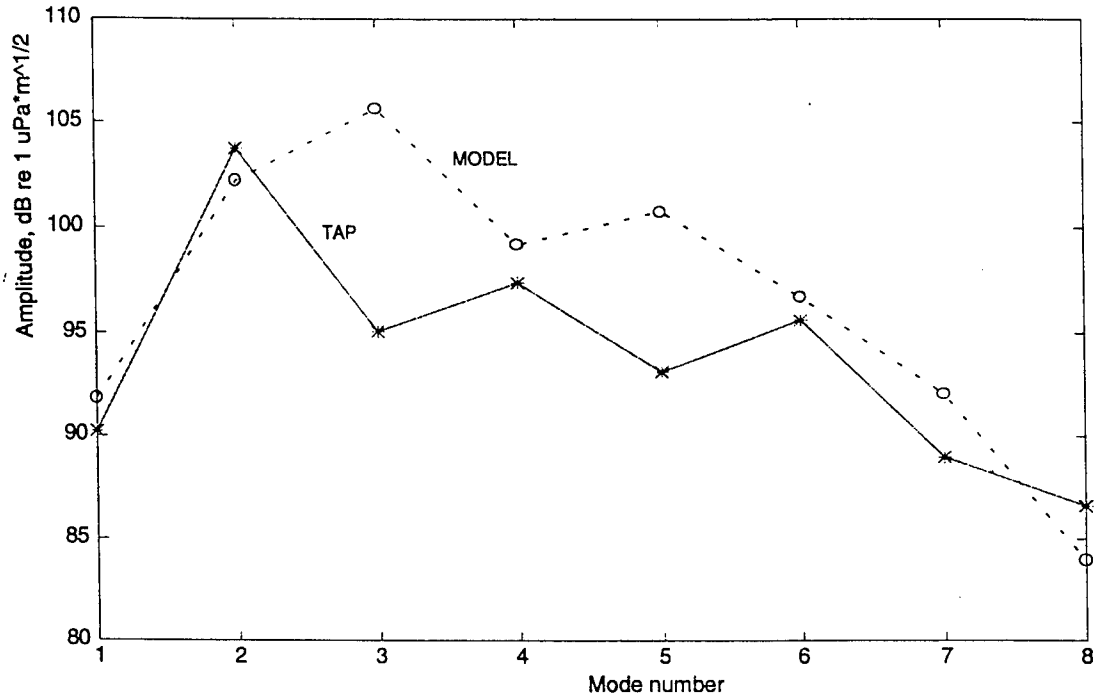

Fig.29. Comparison of the modal amplitudes measured in transmission 31 and computed for the distance of 988.3 km

Table 4. Measured/modeled travel times (in seconds) of modes 1-5 at the path TURPAN-NARWHAL

	Transmission 5	Transmission 19	Transmission 31
Range, km	991.8	990.87	988.3
Mode 1	686.0/687.1	686.4/686.5	684.3/685.0
Mode 2	679.4/681.0	680.2/680.3	678.2/678.9
Mode 3	679.5/681.1	680.2/680.5	677.9/679.0
Mode 4	679.4/681.3	680.2/680.6	677.9/679.2
Mode 5	681.3/681.5	680.4/680.8	-*/679.4

* - the modal arrival peak is split

Table 5. Difference in the modeled and measured travel times (in seconds) of modes 1-4 in signals 5, 19, and 31 received at NARWHAL and SIMI (NARWHAL / SIMI).

Transmission No.	Mode 1	Mode 2	Mode 3	Mode 4
5	1.1/1.6	1.6/2.2	1.6/1.3	1.7/1.3
19	0.1/0.4	0.1/1.2	0.3/0.4	0.4/0.4
31	0.7/0.2	0.7/1.2	1.1/0.5	1.3/0.3

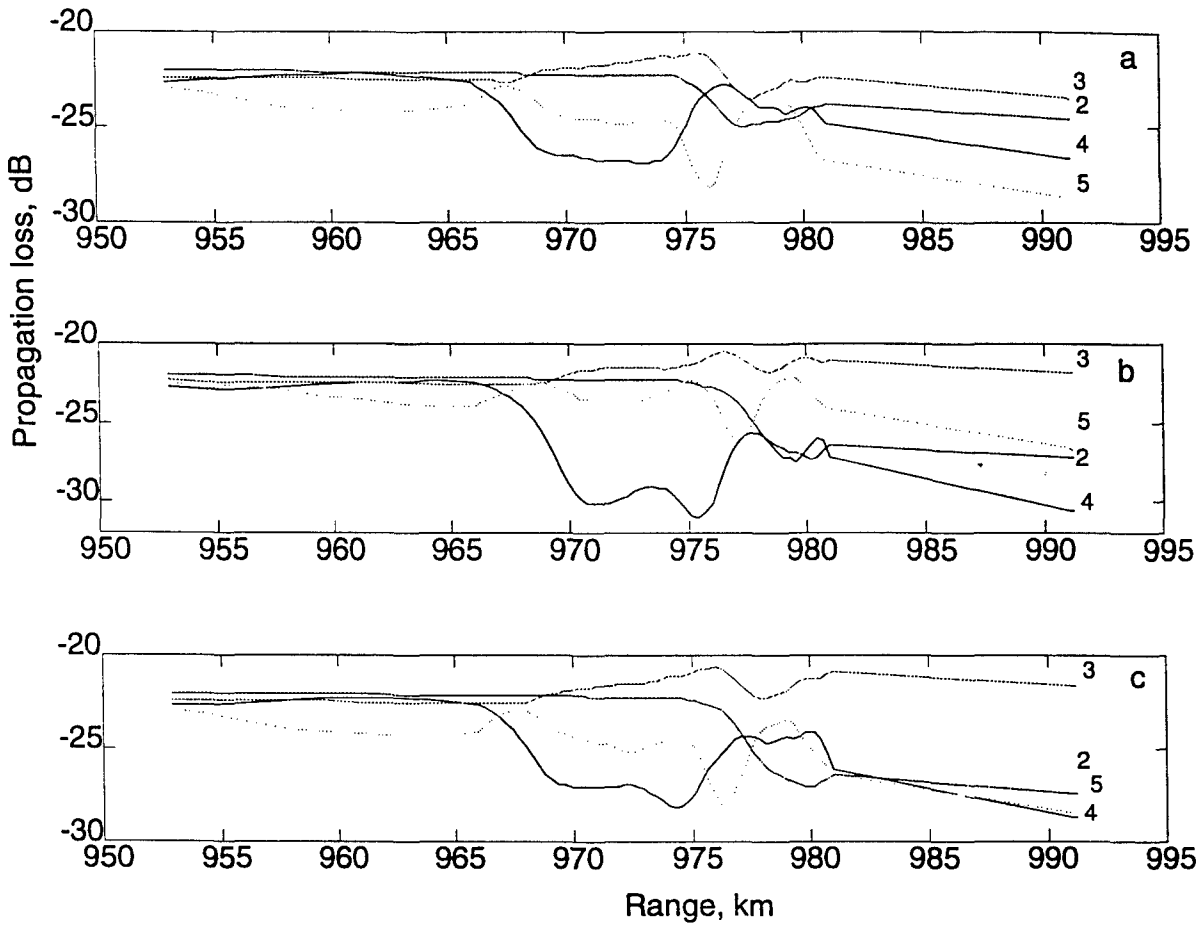

Fig.30. Attenuation of modes 2-5 over the farthest 100 km of the path TURPAN-NARWHAL computed without cylindrical spreading:

a - the same propagation conditions as in Figure 26;

b - same as **a** but for the source displaced by 5 km to NARWHAL;

c - same as **a** but for the sound speed in the Atlantic water core (300--500 m) decreased by 0.5 m/s on average over distances 400-600 km

VI. CONCLUSIONS

Some results of the processing of the TAP signals and ambient noise on the NARWHAL vertical array point to probable errors of a few dB in the array calibration, and also an inconsistency of the actual array gain and some of the records in the operation log.

Spatial filtering of the acoustic modes on the VLA has allowed us to estimate the modal propagation loss. The experimental results are generally in agreement with the results of modeling. The mean modal attenuation coefficients over the path TURPAN-NARWHAL are considerably higher than those on the path TURPAN-SIMI, which is considered to be the result of strong scattering of the acoustic signals by thick and rough ice north of Greenland and in the Lincoln Sea. The results on modal attenuation obtained for the path TURPAN-NARWHAL will be very helpful for planning year-round transarctic transmissions for the ACOUS program with the signal reception in the Lincoln Sea.

However the experimental results show considerable fluctuations in the amplitudes of modes numbered higher 2. Those fluctuations might be caused by changes in the propagation conditions. Variations in the bottom profile along the propagation path over the continental slope due to the drift of the ice camps were probably the main factor of changes in the propagation conditions.

Moreover, the scenario of modal coupling over a sloping bottom depends on the preceding propagation conditions, and, particularly, relative modal phases at the beginning of the irregular waveguide section. Therefore any changes in the waveguide could lead to fluctuations in the modal amplitude, which has been observed in the TAP signals received at NARWHAL.

In broadband signals, the mode phase relations along the propagation path are different for each frequency component. Therefore the modal coupling scenario is also different. This can lead to dissimilar transformation of the spectra of individual modes and, hence, different distortion of the modal pulse form. One of the subjects for future study is how strong are the travel time and phase fluctuations, due to modal coupling, relative to the tomographic response to changes in ocean environment.

REFERENCES

1. P. N. Mikhalevsky, A. B. Baggeroer, A. N. Gavrilov, M. M. Slavinsky, "Experiment tests use of acoustics to monitor temperature and ice in Arctic Ocean", *EOS*, v.**6**, No.27, pp. 265-269, 1955.
2. A. N. Gavrilov, M. Yu. Andreyev, P. N. Mikhalevsky, "Measurements of low-frequency transmission loss in the Transarctic Acoustic Propagation experiment", in Oceans'95 proceeding (CD), 1995.
3. A. N. Gavrilov, M. M. Slavinsky, A. Yu. Shmelerv, "Acoustic thermometry of the Arctic Ocean climate: theoretical and experimental study of feasibility", *UFN*, v.**165**, No.7, pp. 836-840, 1995.
4. B. E. McDonald, M. D. Collins, W. A. Kuperman, K. D. Heaney, "Comparison of data and model predictions for Heard Island acoustic transmissions", *J. Acous. Soc. Am.*, v.**96**, No.4, pp. 2357-2370, 1994.
5. W. H. Geddes, *Geoacoustic model of the Lincoln Sea, GGAI tech. Report* 3-90, 1990.
6. R. Pawlowicz, D. Farmer, B. Sotirin, "Long distance Arctic transmissions to the Lincoln Sea", 1995 (submitted).
7. A. N. Gavrilov, V. M. Kudryashov, "Numerical modeling of long-range low-frequency propagation in an irregular Arctic waveguide", *J. Acous. Soc. Am.*, v.**94**, No.3, Pt.2, p.1770, 1993.
8. R. H. Bourke, A. S. McLaren, "Contour mapping of Arctic Basin ice draft and roughness parameters", *J. Geoph. Res.*, v.**97**, No. C11, pp. 17,715-17,728, 1992.
9. M. A. Dzieciuch, W. H. Munk, "Differential Doppler as a diagnostic", *J. Acous. Soc. Am.*, v.**96**, No.4, pp. 2414-2424, 1994.